Journal of Physics and Chemistry of Solids 69 (2008) 2096–2102

Contents lists available at ScienceDirect

Journal of Physics and Chemistry of Solids

journal homepage: www.elsevier.com/locate/jpcs

Electronic structure, phase stability, and hardness of the osmium borides, carbides, nitrides, and oxides: First-principles calculations

Miao Zhang, Mei Wang, Tian Cui, Yanming Ma *, Yingli Niu, Guangtian Zou

National Lab of Superhard Materials, Jilin University, Changchun 130012, PR China

ARTICLE INFO

Article history:
Received 18 October 2007
Received in revised form
4 March 2008
Accepted 8 March 2008

Keywords:
A. Inorganic compounds
C. *Ab initio* calculations
D. Electronic structure

ABSTRACT

The chemical bonding, elastic behavior, phase stability, and hardness of OsB, OsB_2, OsC, OsO_2, OsN, and OsN_2 have been systematically studied using first-principles calculations. The calculation suggests that the chemical bonding in these compounds is a mixture of covalent and ionic components. The structural stability of OsB, OsC, and OsN can be understood in terms of the band filling of the bonding states, and the results indicate that the hexagonal tungsten carbide structure is more stable. The hardness of these osmium compounds is calculated using both *ab initio* and semiempirical model calculations. Analysis of the *ab initio* hardness suggested that the large occupations and high strength of the covalent bonds are crucial for a superhard material, and there is no clear connection between bulk modulus and hardness in these osmium compounds.

1. Introduction

Superhard materials are particularly useful in a variety of industrial applications, such as abrasives, cutting tools, and coatings due to their superior properties of higher compressional strength, thermal conductivity, refractive index, and chemical stability besides higher hardness [1–4]. Previously, it was commonly accepted that the superhard materials, such as diamond, cubic boron nitride (c-BN), and carbon nitrides, are the strongly covalent bonded compounds formed by light elements [5–7]. However, recently, it was reported that partially covalent heavy transition metal (TM) boride, carbide, nitride, and oxide are found to be good candidates for superhard materials, such as RuO_2 [8] and ReB_2 [9]. Therefore, these pioneering studies open up a novel route for the search of new superhard materials [10–16].

Since the pure osmium (Os) has been found to possess extremely high bulk modulus (>395 GPa) [17,18], its borides, carbides, oxides, and nitrides have, thus, been a topic of much interest to scientists, and are expected to be good candidates for superhard materials. High-pressure X-ray diffraction [11], a scratch test [11], and micro-hardness measurements [17] show that OsB_2 is a low-compressibility material and an ultra-hardness material ($\geqslant 36$ GPa). Later, the bulk moduli of osmium carbide (OsC) and osmium nitride (OsN) in both the hexagonal tungsten carbide (WC) and rocksalt (NaCl) structures have been studied by Zheng [19], who found that they are less compressible in the WC structure. Moreover, the crystal structures and physical properties of osmium borides and nitrides have been extensively studied by Gou et al. [20], Chen et al. [21], and Fan et al. [22]. More recently, using the semiempirical microscopic model, Šimunek and Vackar [23] have investigated the hardness of OsC, OsN, OsB, OsB_2, and OsN_2 within the chosen structures. However, in spite of the existence of a large number of research works, the bonding nature of these compounds is not clear yet, while the discovery of the direct link between bonding behavior and hardness for these compounds is particularly important for future exploration of new superhard materials. Therefore, the investigation of the electronic density of states (DOS), charge density, and chemical bonding is motivated. Moreover, two different models previously proposed are employed in the hardness calculation. Within the calculation errors, it is found that the two theoretical models give practically similar results. The hardness calculation suggests that the large occupation and high strength of covalent bonds are considered as essential for a superhard material.

2. Computational methods and details

The available experimentally determined structure data for the orthorhombic OsB_2 [24] are used as input for the calculation [25]. Previously proposed WC and cesium chloride (CsCl) structures for OsB [20], WC and NaCl structures for OsC and OsN [19–26], and the fluorite structures for OsN_2 and OsO_2 [22] are considered in the calculation. Note that OsB, OsC, and OsN are hypothetical materials at present, which are not successfully synthesized yet by the experiments. Our geometry optimization is performed with

* Corresponding author.
E-mail address: mym@jlu.edu.cn (Y. Ma).

0022-3697/$ - see front matter © 2008 Elsevier Ltd. All rights reserved.
doi:10.1016/j.jpcs.2008.03.008

the Vienna *Ab initio* Simulation Package (VASP) [27–30], applying BlÖchls projector augmented wave (PAW) methods [31,32]. The *k*-point sampling scheme is determined so that the energy is well converged to be better than 1 meV per atom. The electronic calculations are carried out by using the full potential linearized augmented plane wave (LAPW) method [33,34] based on the density-functional theory (DFT) as implemented in the WIEN2k code. The electron exchange-correlation energy is described in generalized gradient approximation (GGA) [35]. Particular care was taken to eliminate the effects of large atomic differences in the choice of the muffin-tin (MT) sphere radius ensuring a reliable calculation. Convergence tests gave the choices of kinetic energy cutoff of $RK_{\max} = 7.0$ and a 3000 *k*-points set in the electronic integration of the Brillouin zone. Elastic constants were obtained from evaluations of the stress tensor generated by small strains using the density-functional plane wave technique as implemented in the CASTEP code [36].

The theoretical hardness of single crystal can be defined as [23]

$$H = \frac{C}{\Omega} n \left[\prod_{i,j=1}^{n} b_{ij} s_{ij} \right]^{1/n} e^{-\sigma f_e}, \quad (1)$$

$$f_e = 1 - \left[k \left(\prod_{i=1}^{k} e_i \right)^{1/k} \Big/ \sum_{i=1}^{k} e_i \right]^2, \quad (2)$$

$$s_{ij} = \sqrt{e_i e_j}/(n_i n_j d_{ij}), \quad (3)$$

where the reference energy e_i is defined as $e_i = Z_i/R_i$, Z_i is the number of valence electrons and R_i is the radius of the sphere (centered at atom i) in which Z_i electrons are contained; n_i and n_j are coordination numbers of atoms i and j, respectively; d_{ij} is the interatomic distance; k corresponds to the number of different atoms in the system, and the exponential factor $\exp(-\sigma f_e)$ is used to denote the effect of the difference between e_i and e_j; s_{ij} is the strength of the individual bond between atoms i and j, b_{ij} is the individual bond in the unit cell. The advantage of this method is that the bond strengths s_{ij}, reflecting the localization of the valence charge around atoms in the bonds, are defined by means of the total charge density of the valence electrons. Therefore, the necessary inputs in Eq. (1) can be calculated directly through the *ab initio* method [37] (here through the LAPW calculations).

For a comparison, the semiempirical hardness model proposed by Gao et al. [15] is also considered in this work. It adopts the following form:

$$H\,(\mathrm{GPa}) = 14(N_a e^{-1.19 f_i}) E_h = 8.82(N_e^{2/3} e^{-1.19 f_i}) E_h, \quad (4)$$

where E_h is the covalent gap which characterizes the strength of the covalent bond, N_a the covalent bond number per unit area, f_i the ionicity of bonds, and N_e the electron density expressed in the number of valence electrons per cubic angstrom.

3. Results and discussion

We compute the equilibrium lattice constants and the bulk moduli B_0 by fitting the energy–volume curves to the third order Birch–Murnaghan equation-of-state (EOS). The bulk moduli B_0 with GGA and the local density approximation (LDA) [38] for the exchange-correlation energy functional as well as the equilibrium lattice parameters are listed in Table 1. It can be seen clearly that the calculated lattice parameters for all the osmium compounds are in satisfactory agreement with the previous calculations and available experimental data. It is understandable that the LDA B_0 is larger than that of GGA due to the predicted smaller lattice volume in LDA. Note that the bulk moduli of the osmium compounds are all very large to be in the range of 303–376 GPa for GGA and 334–424 GPa for LDA, respectively. However, most of them are smaller than that (395–460 GPa) of Os due to the addition of the B, C, N, or O atoms [26]. The complete set of zero-pressure elastic constants for all the compounds is shown in Table 2. The elastic stability is checked by the whole set of elastic stiffness constants c_{ij} that satisfies all the below conditions by using Born–Huang criterion [39,40]. The key criterion for mechanical stability of a crystal is that strain energy must be positive [41]. This means in a cubic crystal that the elastic constants should satisfy the following inequalities:

$$c_{44} > 0, \quad c_{11} > |c_{12}|, \quad c_{11} + 2c_{12} > 0, \quad (5)$$

while for a hexagonal crystal

$$c_{44} > 0, \quad c_{11} > |c_{12}|, \quad (c_{11} + c_{12}) c_{33} > 2c_{13}^2. \quad (6)$$

According to the above criteria, it is clear that OsC and OsN within the NaCl structure are unstable at the ambient condition. Based on elastic constants, the bulk modulus (B), the shear modulus (G), the Young's modulus (E) and the Poisson's ratio (ν) in cubic crystals can be deduced as [13]: $B = (c_{11}+2c_{12})/3$, $G = (c_{11}-c_{12}+2c_{44})/4$, $E = 9BG/(3B+G)$, and $\nu = E/(2G)-1$, respectively. The calculated results of the cubic osmium compounds are shown in Table 2.

The elastic anisotropy of crystals has an important implication in engineering science since it is highly correlated with the possibility to induce microcracks in the materials [42]. Hence it is desirable to obtain the elastic anisotropy in understanding the physical properties of certain materials. For cubic crystals, the anisotropy factor can be defined as $A = (2c_{44}+c_{12})/c_{11}$ [42,43]. If A takes the value of 1 it denotes a completely isotropic material, while values smaller or greater than unity measure the degree of elastic anisotropy. Here, for the elastic stable cubic OsB, OsN_2, and OsO_2 crystals the anisotropy factors are calculated to be 0.38, 0.97, and 0.93, respectively. The current results demonstrate that OsN_2 and OsO_2 are strongly isotropic, while OsB with CsCl structure has a strong characteristic of anisotropy.

We inspect the electronic DOS of OsB, OsC, and OsN as plotted in Fig. 1 to understand the chemical bonding between Os and the light elements (B, C, and N) and to probe the phase stabilities for the choices of the WC and CsCl/NaCl structures. The DOS shows large similarities in the three compounds. First of all, they indicate metallic behavior by evidence of finite DOS, $N(E_F)$, at the Fermi level, which are listed in Table 3. Secondly, it was found that the electronic structures of these compounds are governed by a strong hybridization between the Os-d and B (C or N)-p states. The bonding and antibonding states are located at the bottom and top of the p–d complex, with the nonbonding d states in between, where little overlapping (or hybridizing) can be seen between Os-d and B (C or N)-p states [44]. It should be noted that the covalent interactions in OsB for both WC-type and CsCl-type are relatively small since the mixture between Os-d and B-p DOS states is somewhat obscure. So it is reasonable that one can take the approximate valleys as the separation for bonding, nonbonding, and antibonding regions. Based on the definition of pseudogap [45,46], i.e., the valley between bonding and nonbonding (or antibonding) states, the pseudogaps of the osmium compounds are found to locate at ~ -1.06 and -1.47 eV for WC-type and CsCl-type OsB, -2.49 and -3.69 eV for WC-type and NaCl-type OsC, and -2.93 and -4.54 eV for WC-type and NaCl-type OsN (Fig. 1), respectively. As proposed by Gelatt et al. [44–47], there are two factors that mainly contribute to the phase stability of the osmium compounds: (i) the hybridization between the Os-d states and the B (C or N)-p states; (ii) the weakening of the bonding between Os atoms which results from the insertion of light elements. In the nonbonding region, the second factor dominates over the first.

Table 1
Calculated equilibrium lattice parameters and bulk moduli B_0 for the osmium compounds studied

	a_0 (Å)	b_0 (Å)	c_0 (Å)	B_0 (GPa)
OsB(WC)				
GGA	2.899(2.888[a])		2.878(2.859[a])	351.9(350[a])
LDA	2.863(2.857[a])		2.856(2.840[a])	393.6(383[a])
OsB(CsCl)				
GGA	2.728(2.713[a])			363.5(363[a])
LDA	2.698(2.688[a])			403.6(389[a])
OsC(WC)				
GGA	2.951(2.928[b])		2.728(2.717[b])	375.6(396[b])
LDA	2.914		2.700	424.4
OsC(NaCl)				
GGA	4.361(4.333[b])			355.6(366[b])
LDA	4.308(4.33[c])			403.9(392[c])
OsN(WC)				
GGA	2.755(2.743[b])		3.138(3.100[b])	342.9(367[b])
LDA	2.708		3.097	405.9
OsN(NaCl)				
GGA	4.367(4.335[b])			325.5(342[b])
LDA	4.298(4.32[c])			385.8(372[c])
OsB_2				
GGA	4.702(4.664[a])	2.889(2.867[a])	4.091(4.074[a])	302.9(307[a])
LDA	4.652(4.636[a], 4.6433[d])	2.853(2.842[a], 4.8467[d])	4.052(4.044[a], 4.0432[d])	334.1(332[a], 365[d])
Expt	4.683[e]	4.683[e]	4.076[e]	365–395[e]
OsN_2(fluorite)				
GGA	4.876(4.856[f], 4.834[g])			332.9(333.3[f], 341[g])
LDA	4.805(4.781[f], 4.781[g])			388.0(388.0[f], 386[g])
OsO_2(fluorite)				
GGA	4.880(4.861[f])			316.0(316.7[f])
LDA	4.792(4.770[f])			380.9(378.2[f])

[a] Ref. [20].
[b] Ref. [19].
[c] Ref. [26].
[d] Ref. [52].
[e] Ref. [10].
[f] Ref. [22].
[g] Ref. [53].

Table 2
Calculated elastic constants c_{ij} (GPa), shear modulus G, Young's modulus E, Poisson's ratio v for the osmium compounds

	c_{11}	c_{22}	c_{33}	c_{44}	c_{55}	c_{66}	c_{12}	c_{13}	c_{23}	G (GPa)	E (GPa)	v
OsB (WC)	619		782	193			189	176				
OsB (CsCl)	764			65			159			184	471	0.28
OsC (WC)	216		813	39			170	129				
OsC (NaCl)	456			−91			251			6	17	0.49
OsN (WC)	268		670	163			101	108				
OsN (NaCl)	317			−239			296			−114	−392	0.72
OsB_2	622	609	914	225	185	314	176	227	124		314	
OsN_2	456			95			254			98(89.4[a])	274(246.2[a])	0.40(0.38[a])
OsO_2	678			226			181			237(223.9[a])	579(543.6[a])	0.22(0.21[a])

[a] Ref. [22].

According to the band filling theory [46–49], filling bonding or antibonding/nonbonding states will increase or reduce the cohesion (or stability). To evaluate the band-filling situation, we apply the definitions of W_{occ} (the width of the occupied states) and W_b (the width of the bonding states) as the distances from the bottom of the band to E_F and to the pseudogap, respectively. Thus, W_{occ}/W_b can be taken to describe the occupied portion of the bonding states [46]. The phase is expected to be more stable when the W_{occ}/W_b value is closer to 1.0. For the three osmium compounds, the calculated W_{occ}, W_b and W_{occ}/W_b, are listed in Table 3. It can be clearly seen that the W_{occ}/W_b value of OsB within the WC structure reaches 1.09, which is 0.03 lower than that in the CsCl structure; similarly, W_{occ}/W_b values in the WC-type OsC and OsN are 1.30 and 1.36, respectively, which are 0.32 and 0.44 more closer to 1.0 than those in the NaCl structure. These results demonstrate that the choices of the WC structure for OsB, OsC, and OsN are more preferable.

The calculated $N(E_F)$, total energy ($-E$), and the cohesive energy for OsC, OsN, and OsB are also listed in Table 3. It is apparent that the total energies of the three compounds within the WC structure are much lower, signifying the energetically favorable structure nature. Thus, the current total energy calculations strongly support the above band-filling analysis. Moreover, it is interesting to note that the stable structure is associated with a lower $N(E_F)$ [46–50]. For the more stable structure, there is always a tendency to accommodate all its valence electrons into the bonding states so as to bring the Fermi level to a valley position separating bonding and nonbonding (or antibonding) [48], thus

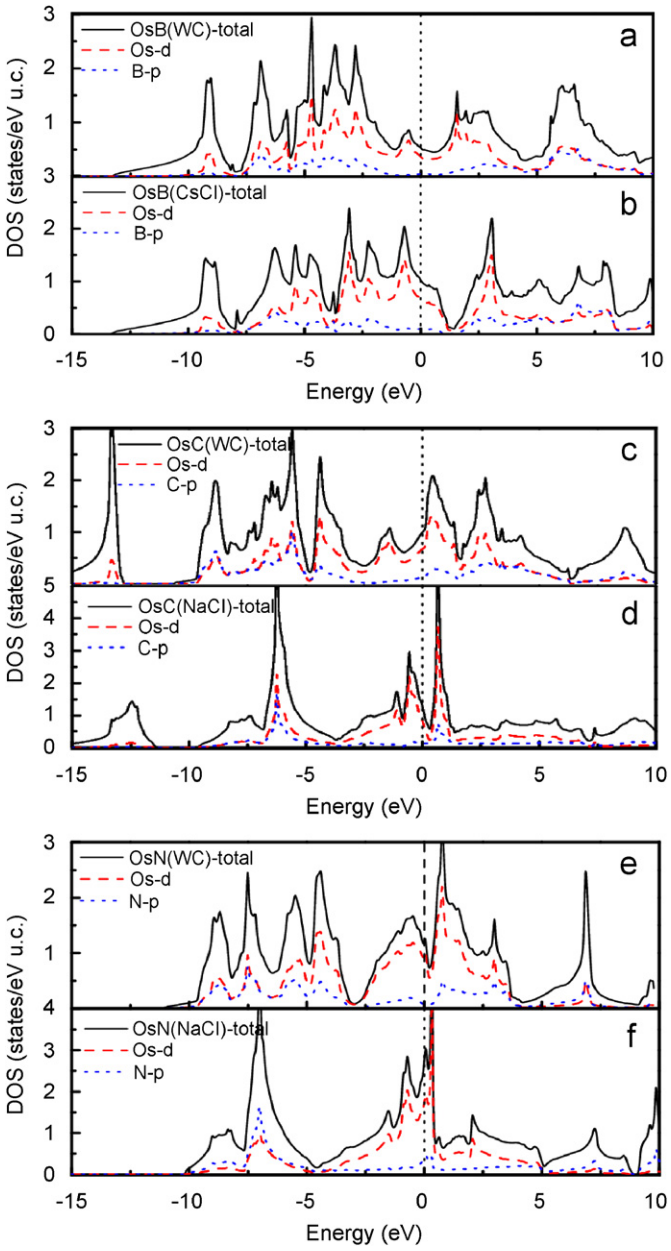

Fig. 1. (Color online) Total and site projected density of states for OsB, OsC and OsN, respectively. (a) OsB in WC structure; (b) OsB in CsCl structure; (c) OsC in WC structure; (d) OsC in NaCl structure; (e) OsN in WC structure; (f) OsN in NaCl structure.

Table 3
The width of the occupied states (W_{occ}) and the bonding states (W_b), W_{occ}/W_b, total density of states at E_F [$N(E_F)$] (in states/eV cell), the total energy ($-E$) (in Ry/f.u.) and the cohesive energy (E_{coh}) of OsB, OsC, and OsN in the WC and CsCl (or NaCl) structures, respectively

	W_{occ}	W_b	W_{occ}/W_b	$N(E_F)$	$-E$	E_{coh}
OsB						
WC	13.24	12.18	1.09	0.51	34613.659	11.07
CsCl	13.30	11.83	1.12	1.02	34613.592	10.61
OsC						
WC	10.64	8.15	1.30	1.00	34639.999	10.72
NaCl	9.62	5.93	1.62	1.23	34639.955	10.42
OsN						
WC	11.05	8.12	1.36	1.20	34673.262	9.02
NaCl	10.25	5.71	1.80	2.81	34673.234	8.83

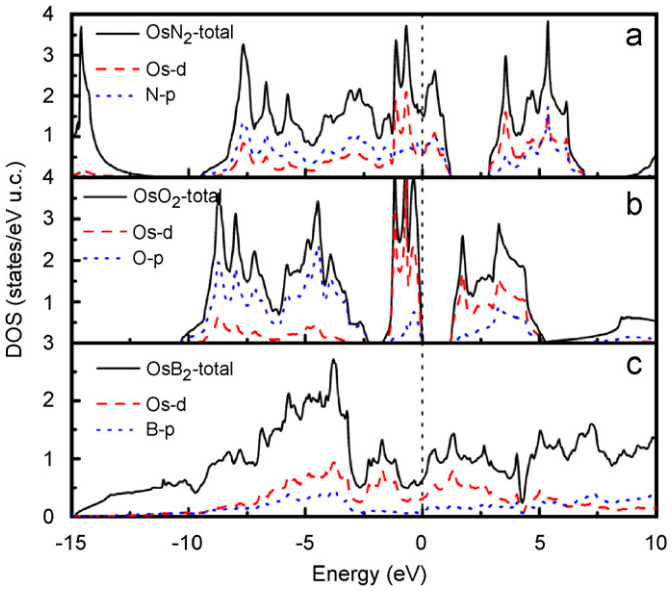

Fig. 2. (Color online) Total and site projected density of states for OsN_2 (a), OsO_2 (b), and OsB_2 (c), respectively.

preferring a lower $N(E_F)$. It is noteworthy that the stable WC structures for these compounds possess larger cohesive energies as listed in Table 3.

Fig. 2 shows the electronic DOS for OsB_2, OsN_2, and OsO_2. A clear covalent chemical bonding is also evidenced between Os and N, B, and O, respectively. Note that the covalent interactions in OsB_2, OsN_2, and OsO_2 are obviously larger than those in OsB, OsC, and OsN resulting from the larger Os-N (B and O) overlaps in the DOSs shown in Fig. 2. Interestingly, OsO_2 shows an insulating feature, which is unique in the studied osmium compounds.

In order to further understand the bonding behaviors of the stable osmium compounds, the difference charge density contour plots in the chosen planes are shown in Fig. 3. It is known that the changes in the original atomic density distributions caused by the formation of the chemical bond may be isolated and studied directly by the construction of a density difference distribution. Such a distribution is obtained by subtracting the density obtained from the overlap of the undistorted atomic densities separated by a distance R, from the molecular charge distribution evaluated at the same value of R. Wherever this density difference is positive (negative) in value it means that the electron density in the molecule is greater (less) than that obtained from the overlap of the original atomic densities. Such a density difference map thus provides a detailed picture of the net reorganization of the charge density of the separated atoms accompanying the formation of a molecule. From Fig. 3, one clearly observes that the formation of the osmium compounds results in an electron transfer from Os to the light elements, signifying an ionic bonding feature of these compounds. It is worth noting that the charge accumulation along the bonding directions between Os and the light elements is an indication of covalent bonding. From Fig. 3, it is evident that there are more covalent bondings in the light-element-rich compounds due to the involvement of more light elements, as also supported in the electronic DOS calculations (Figs. 1 and 2). Notably, the heavier charge accumulations in OsN_2, OsO_2, and OsB_2 represent a stronger covalent bonding feature than those in OsC, OsN, and OsB. Interestingly, two neighbor B atoms in OsB_2 (Fig. 3f) are found to form a covalent bond, making this material peculiar.

The hardness of the osmium compounds studied in this work is systematically explored using both *ab initio* [37–51] and

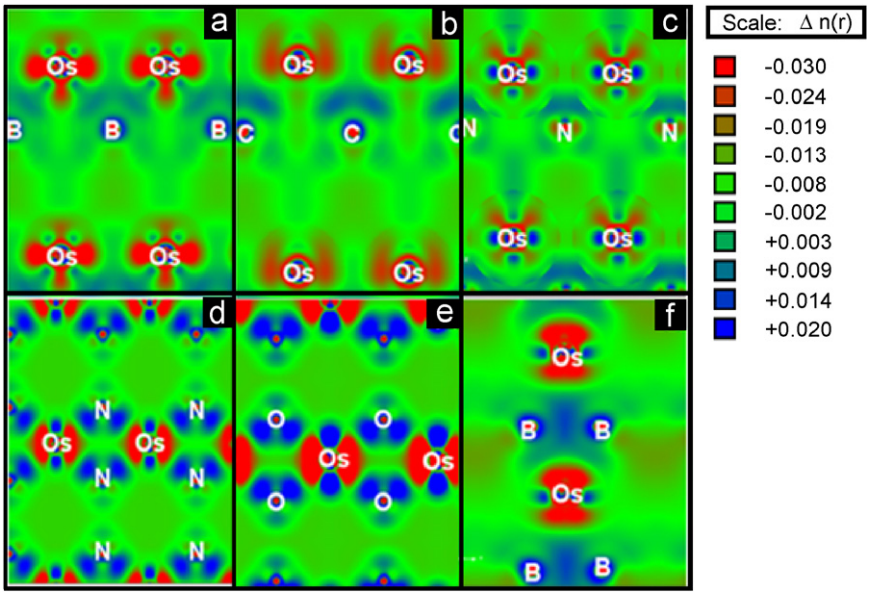

Fig. 3. (Color online) The difference charge density contour (e/Å^3) plots for OsB (a), OsC (b), and OsN (c) within the WC structure in (1 1 0) plane; OsN_2 (d) and OsO_2 (e) in (0 1 $\bar{1}$) plane; OsB_2 (f) in (0 1 0) plane.

Table 4
Hardness and parameters related to the hardness calculations of the osmium compounds, where H_{theor} and H_{Gao} are the calculated hardness using two methods of *ab initio* and semi-empirical, respectively

	d (Å)	Ω	f_e	S_{ij}	H_{theor} (GPa)	N_e	E_h	E_g	f_i	H_{gao} (GPa)
OsB (WC)	2.195	20.567	0.0430	0.0425	16.2 (18.5[a])	0.535	5.66	7.96	0.495	18.2
OsB (CsCl)	2.363	20.317	0.0539	0.0217	10.7	0.541	4.71	7.98	0.652	12.7
OsC (WC)	2.169	20.175	0.0022	0.0508	23.2 (24.3[b,a])	0.595	5.83	7.33	0.368	23.4
OsC (NaCl)	2.181	20.754	0.0016	0.0500	22.2 (24.1[a])	0.578	5.75	7.25	0.373	22.5
OsN (WC)	2.216	20.198	0.0067	0.0556	25.0 (25.9[a])	0.644	5.52	6.28	0.225	27.7
OsN (NaCl)	2.179	20.703	0.0093	0.0567	24.6 (26.3[a])	0.628	5.76	6.59	0.237	28.0
OsB_2	2.221	27.161	0.0324	0.0270[a]	32.5 (35.5[a])					
OsN_2	2.070	27.322	0.0057	0.0687	30.5 (29.8[a], 35.9[a])	0.659	6.54	6.88	0.096	38.9
OsO_2	2.065	27.134	0.0221	0.0966	40.4	0.737	6.58	7.74	0.278	34.0

Note: We use the method described in Ref. [37] to yield the current H_{theor} results.
[a] Refs. [23,37].
[b] Bond strength of Os–B bonding.

semiempirical methods [15] as listed in Table 4. The current *ab initio* results are in satisfactory agreement with the previous semiempirical calculations by Šimůnek [23]. It is significant that the introduction of light elements into Os is crucial to "harden" it. It is previously reported that the hardness of Os is 3.92 GPa [17], which is much smaller than those in the osmium compounds as listed in Table 4. It is clear that the addition of light elements to Os results in the formation of the covalent bonding between Os and light elements, which is a key factor for the material hardness. Moreover, it is noteworthy that the hardness values (<30 GPa) for OsC, OsN, and OsB within the chosen structures are all smaller than those (>30 GPa) in the light-element-rich compounds of OsN_2, OsO_2, and OsB_2. This fact is mainly due to the involvement of more and stronger covalent bonds in OsN_2, OsO_2, and OsB_2 as indicated in Figs. 2 and 3. From Table 4, it is also found that within one osmium compound the different structure choices give similar hardness values. In view of the small local structure changes within the choices of WC and CsCl/NaCl structures, it is indicated that small modifications of local structure will not alter significantly the hardness. It is worth noting that the largest theoretical hardness within the first-principles method is calculated to be 40.4 for OsO_2, which is much smaller than that of 93.6 GPa [15] in diamond. Note that none of the hardness in other compounds is found to be beyond 40 GPa, a critical value to define a superhard material. Moreover, previously, there were extensive debates on the validity of the theoretical model in the hardness calculation [51]. However, from the current calculations (Table 4), the two hardness models essentially give similar hardness values in spite of the fact that the semiempirical model is designed for typical covalent and polar covalent crystals [15].

Traditionally, it is generally accepted that high bulk modulus materials might not be hard materials. Here we provide the direct evidence for this conclusion. The direct comparison of hardness (Table 4) and the bulk moduli (Table 1) demonstrates that there is no clear relationship between hardness and bulk modulus. Therefore, one must use the language of large bulk modulus with particular cautions in representing the large hardness. Specifically, from the current calculation it is found that the WC-type OsB and OsC both possess very large bulk moduli above 350 GPa, while the corresponding hardness values are as small as 16.2 and 23.2 GPa from the *ab initio* calculations, and 18.2 and 23.4 GPa from the semiempirical model. Here, if we only consider the *ab initio* model in the hardness calculation, it is interesting to note that there is an obvious hardness trend in the sequence of CsCl OsB→WC OsB→

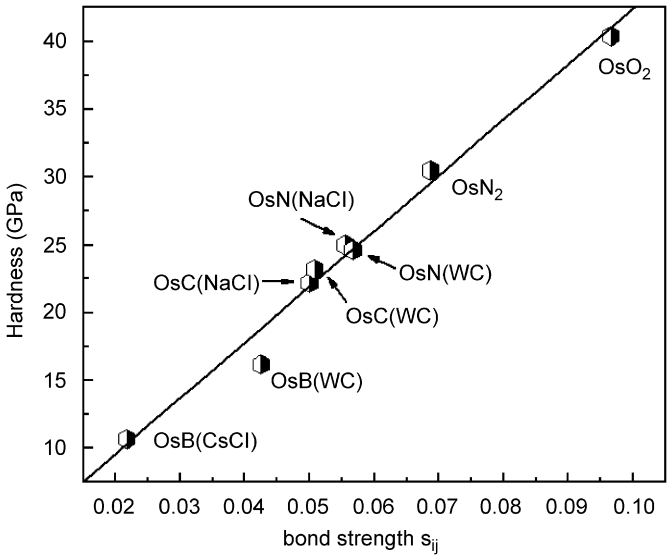

Fig. 4. Correlation of hardness and bond strength for the osmium compounds.

WC OsC → NaCl OsC → WC OsN → NaCl OsN → orthorhombic OsB_2 → fluorite OsN_2 → fluorite OsO_2 as listed in Table 4. Fig. 4 shows the variation of the hardness with the bond strength. Significantly, it is indicated that the bond strength S_{ij}, as listed in Table 4, is the dominating factor for the hardness in the osmium compounds. From the definition of the bond strength in Eq. (3), it is a reflection of localized charge in the bond. In principle, the bond strength is a good measure of the strength of the covalent bonding. Therefore, the calculations suggest strongly that the strength of the covalent bonds in osmium compounds has significant contributions to the hardness. Compared with other osmium compounds, OsB in both WC and CsCl structures exhibits the smallest bond strength S_{ij} (except for OsB_2 with two types of bonds), i.e., the weakest covalent bonding, which can be also evidenced from the DOS curves (Fig. 1) as mentioned before and the difference charge density plot (Fig. 3). Also, the calculated ionicity f_i scaled by Phillips (as listed in Table 4) demonstrates that the bonding of OsB is more ionic than others. The weak covalent bonding in OsB is suggested to be responsible for its small hardness. The current discovery of the direct link of covalent bonding with the hardness might shed strong light on the future design of new superhard materials.

4. Conclusion

In summary, we have presented a complete theoretical analysis of the structural, electronic, elastic, and chemical bonding properties of osmium borides, carbides, nitrides, and oxides using first-principles calculations. The bonding nature of these osmium compounds is investigated via the density of states histogram and the charge density plots to be a mixture of covalent and ionic components. The structural stability of OsB, OsC, and OsN is analyzed using the band filling principle. The hardness of these osmium compounds is calculated using both *ab initio* and semiempirical model calculations. The two methods give essentially similar results. Our calculations indicate that these osmium compounds are ultraincompressible, but not superhard, in good agreement with the results of Ref. [37]. It should be emphasized that the current work discovers a direct link between the covalent bonding and the hardness, which is helpful for the future design of new superhard materials.

Acknowledgments

We would like to thank the financial support of the NSAF of China (no. 10676011), the China 973 Program under Grant no. 2005CB724400, the NDFCEM (no. 20050183062), the SRF for ROCS, SEM, the Program for 2005 New Century Excellent Talents in University, and the 2006 Project for Scientific and Technical Development of Jilin Province.

References

[1] A.G. Thornton, J. Wilks, Nature (London) 274 (1978) 792.
[2] A. Szymanski, J.M. Szymanski, Hardness Estimation of Minerals Rocks and Ceramic Materials, Elsevier, Amsterdam, 1989.
[3] I.J. McColmm, Ceramic Hardness, Plenum Press, London, 1990.
[4] J.J. Gilman, in: J.H. Westbrook, H. Conrad (Eds.), The Science of Hardness Testing and Its Research Applications, ASM, Ohio, 1973.
[5] J. Haines, J.M. Léger, G. Bocquillon, Annu. Rev. Mater. Res. 31 (2001) 1.
[6] A.Y. Liu, M.L. Cohen, Science 245 (1989) 841.
[7] G.-M. Rignanese, J.-C. Charlier, X. Gonze, Phys. Rev. B 66 (2002) 205416.
[8] K. Benyahia, Z. Nabi, A. Tadjer, A. Khalfi, Physica B 339 (2003) 1;
J.S. Tse, D.D. Clug, K. Uehara, Z.Q. Li, J. Haines, J.M. Léger, Phys. Rev. B 61 (2000) 10029;
J. Haines, J.M. Léger, M.W. Schmidt, J.P. Petitet, A.S. Pereira, J.A.H. Da Jornada, S. Hull, J. Phys. Chem. Solids 59 (1998) 239.
[9] H.Y. Chung, M.B. Weinberger, J.B. Levine, A. Kavner, J.M. Yang, S.H. Tolbert, R.B. Kaner, Science 316 (2007) 436.
[10] R.W. Cumberland, M.B. Weinberger, J.J. Gilman, S.M. Clark, S.H. Tolbert, R.B. Kaner, J. Am. Chem. Soc. 127 (2005) 7264.
[11] R.B. Kaner, J.J. Gilman, S.H. Tolbert, Science 308 (2005) 1268.
[12] A.F. Young, C. Sanloup, E. Gregoryanz, S. Scandolo, R.J. Hemley, H.K. Mao, Phys. Rev. Lett. 96 (2006) 155501.
[13] A.Y. Liu, R.M. Wentzcovitch, M.L. Cohen, Phys. Rev. B 38 (1988) 9483.
[14] V.L. Solozhenko, D. Andrault, G. Fiquet, M. Mezouar, D.C. Rubie, Appl. Phsys. Lett. 78 (2001) 1385.
[15] F.M. Gao, J.L. He, E.D. Wu, S.M. Liu, D.L. Yu, D.C. Li, S.Y. Zhang, Y.J. Tian, Phys. Rev. Lett. 91 (2003) 015502.
[16] S. Chiodo, H.J. Gotsis, N. Russo, E. Sicilia, Chem. Phys. Lett. 425 (2006) 311–314.
[17] M. Hebbache, M. Zemzemi, Phys. Rev. B 70 (2004) 224107.
[18] H. Cynn, J.E. Klepeis, Choong-Shik Yoo, D.A. Young, Phys. Rev. Lett. 88 (2002) 135701.
[19] J.C. Zheng, Phys. Rev. B 72 (2005) 052105.
[20] H.Y. Gou, L. Hou, J.W. Zhang, H. Li, G.F. Sun, F.M. Gao, Appl. Phys. Lett. 88 (2006) 221904.
[21] Z.W. Chen, X.J. Guo, Z.Y. Liu, M.Z. Ma, Q. Jing, G. Li, X.Y. Zhang, L.X. Li, Q. Wang, Y.J. Tian, R.P. Liu, Phys. Rev. B 75 (2007) 054103.
[22] C.Z. Fan, S.Y. Zeng, L.X. Li, Z.J. Zhan, R.P. Liu, S.Y. Zeng, Phys. Rev. B 74 (2006) 125118.
[23] A. Šimunek, J. Vackar, Phys. Rev. Lett. 96 (2006) 085501.
[24] R.B. Roof, R.J. Fries, C.P. Kempeterm, J. Chem. Phys. 37 (1962) 1473.
[25] P. Blaha, K. Schwarz, G.K.H. Madsen, D. Kvasnicka, J. Luitz, WIEN2k, An Augmented Plane Wave+Local Orbitals Program for Calculating Crystal Properties, Karlheinz Schwarz, Techn. Universität Wien, Austria, ISBN 3-9501031-1-2, 2001.
[26] J.C. Grossman, A. Mizel, M. Cote, M.L. Cohen, S.G. Louie, Phys. Rev. B 60 (1999) 6343.
[27] G. Kresse, J. Hafner, Phys. Rev. B 47 (1993) 558.
[28] G. Kresse, J. Hafner, Phys. Rev. B 49 (1994) 14251.
[29] G. Kresse, J. Furthmüller, Comput. Mater. Sci. 6 (1996) 15.
[30] G. Kresse, J. Furthmüller, Phys. Rev. B 54 (1996) 11169.
[31] P.E. Blöchl, Phys. Rev. B 50 (1994) 17953.
[32] G. Kresse, D. Joubert, Phys. Rev. B 59 (1999) 1758.
[33] M. Hebbache, L. Stuparević, D. Živković, Solid State Commun. 139 (2006) 227.
[34] D.J. Singh, Planewaves, Pseudopotentials and the LAPW Method, Kluwer Academic, 1994.
[35] J.P. Perdew, K. Burke, Int. J. Quantum Chem. 57 (1996) 309;
J.P. Perdew, K. Burke, M. Ernzerhof, Phys. Rev. Lett. 77 (1996) 3865.
[36] MATERIALS STUDIO, Version 2.1.5, Accelrys Inc., San Diego, CA, 2002;
M.D. Segall, P.L.D. Lindan, M.J. Probert, C.J. Pickard, P.J. Hasnip, S.J. Clark, M.C. Payne, J. Phys.: Condens. Matter 14 (2002) 2717.
[37] A. Šimůnek, Phys. Rev. B 75 (2007) 172108.
[38] D.M. Ceperley, B.J. Alder, Phys. Rev. Lett. 45 (1980) 566.
[39] M. Born, Proc. Cambridge Philos. Soc. 36 (1940) 160.
[40] M. Born, K. Huang, Dynamical Theory of Crystal Lattices, Clarendon, Oxford, 1956.
[41] J.F. Nye, Physical Properties of Crystals, Oxford University Press, Oxford, 1985.
[42] M. Mattesini, R. Ahuja, B. Johansson, Phys. Rev. B 68 (2003) 184108.
[43] B.B. Karki, L. Stixrude, S.J. Clark, M.C. Warren, G.J. Ackland, J. Crain, Am. Mineral. 82 (1997) 51.
[44] C.D. Gelatt Jr., A.R. Williams, V.L. Moruzzi, Phys. Rev. B 27 (1983) 2005.

[45] A. Pasturel, C. Colinet, P. Hicter, Physica B+C 132B (1985) 177.
[46] J.-H. Xu, A.J. Freeman, Phys. Rev. B 40 (1989) 1927.
[47] A.R. Williams, C.D. Gelatt Jr., J.W.D. Connolly, V.L. Moruzzi, in: L.H. Bennett, T.B. Massalski, B.C. Giessen (Eds.), Alloy Phase Diagrams, North-Holland, New York, 1983, p. 17.
[48] J.-H. Xu, A.J. Freeman, Phys. Rev. B 41 (1990) 12553.
[49] C. Colinet, A. Pasturel, K.H.J. Bushow, Physica B (Amsterdam) 150 (1988) 397.
[50] J.-H. Xu, T. Oguchi, A.J. Freeman, Phys. Rev. B 35 (1987) 6940.
[51] Z.Y. Liu, X. Guo, J. He, D. Yu, Y. Tian, Preceding comment, Phys. Rev. Lett. 98 (2007) 109601;
A. Šimunek, J. Vackar, Phys. Rev. Lett. 98 (2007) 109602.
[52] Z.Y. Chen, H.J. Xiang, J.L. Yang, J.G. Hou, Q.S. Zhu, Phys. Rev. B 74 (2006) 012102.
[53] Z.J. Wu, X.F. Hao, X.J. Liu, J. Meng, Phys. Rev. B 75 (2007) 054115.